C98/75

ANALYSIS OF PERFORMANCE LOSSES IN A WANKEL ENGINE

G. A. DANIELI,
C. R. FERGUSON,
J. B. HEYWOOD,
J. C. KECK
Department of Mechanical Engineering, Massachusetts Institute of Technology
The Ms. of this paper was received at the Institution on 13th January 1975 and accepted for publication on 18th March 1975

ABSTRACT A performance model of a Wankel engine has been developed which predicts the mass fraction burned in the combustion chamber as a function of chamber pressure. The model includes gas leakage past the seals, heat transfer, and flame quenching on the chamber walls and at the entrance to crevices. Experiments were performed on a production Wankel engine to obtain chamber pressure-time diagrams, and engine performance and emissions data. The uniformity of the mixture in the chamber was studied by time resolving the exhaust mass flow rate and the exhaust concentrations of unburned hydrocarbons, carbon monoxide, nitric oxide, oxygen, and carbon dioxide. No evidence of charge stratification was observed. Model predictions of mass burnt, global heat transfer, and hydrocarbon emissions are in good agreement with measurements. The model is then used in a parametric study of thermal efficiency as a function of an effective leakage area, and the effects of finite burning angle, heat transfer and wall quench on efficiency are assessed.

INTRODUCTION

1. The problem addressed in this paper is that of performance losses in a Wankel engine. A theoretical analysis capable of a priori predictions is not yet plausible because the mechanisms of flame propagation and the structure of fluid motions in internal combustion engines are not adequately understood, though progress is being made [1,2]. In the studies described here, a measured pressure diagram is used to bypass the modeling of the flame propagation process [3]. An alternate approach would be to use an empirical burning law [4, 5] which has the advantage of allowing extrapolation to conditions different from the experiments. However, it is important to recognize that assumptions concerning the flame speed will affect the calculated engine performance. Observations of flame propagation within Wankel engines show the flame speed is fastest in the direction of rotor rotation [6, 7]. It is believed that gas motion from the trailing zone of the combustion chamber to the leading zone is responsible for this effect. It is also believed that these gas motions are in part responsible for rich portions of the charge concentrating at the trailing side of the combustion space [8]. The model developed here assumes a homogeneous change, and experimental evidence is presented to support that assumption.

2. The performance model outlined here was developed to quantify performance losses which result from heat transfer, seal leakage, and flame quenching. All these phenomena are treated approximately. Our object is twofold: to give a tolerably complete picture of performance losses in a Wankel engine and to use that information to evaluate performance gains realizable by leakage reduction. While there has been much discussion of the Wankel engine and its performance characteristics, there has been little effort devoted to quantifying the relative importance of the different loss mechanisms.

3. LIST OF SYMBOLS

a	sound speed
A	area
c	constant
c_v	constant volume specific heat
h_f	specific enthalpy of formation of absolute zero
H	integral loss of extensive enthalpy from open system
m	mass
Nu	Nusselt number
p	Pressure
Q	integral heat loss by a system
q	quench layer thickness
r	generating radius
Re	Reynolds number
t	time
T	temperature
v	velocity
V	volume
W	integral work done by a system
x	mass fraction burned
α, β	coefficients in quench correlation
γ	specific heat ratio

LIST OF SYMBOLS (cont.)

δ finite difference operator

ρ density

ψ surface to volume ratio

ω angular velocity of crank shaft

SUBSCRIPTS

b burned

d displacement

f flame

j upstream chamber

k downstream chamber

ℓ leakage per apex seal

m motoring

o ignition

q quenched

qc quench crevice cross section

r reference condition

u unburned

w wall

SUPERSCRIPTS

* critical (sonic)

—— average

PERFORMANCE MODELS

4. The analysis uses a measured chamber pressure-time diagram to eliminate the closure problem which, as mentioned, results from an incomplete understanding of the processes governing turbulent flame propagation. Mass and energy conservation equations are then applied to open systems (Fig. 1) defined by the three instantaneous chamber volumes in any one rotor, to calculate the engine performance characteristics [9]. The equations used to estimate the three important loss mechanisms--wall quenching, leakage past the seals, and heat transfer will now be reviewed.

(a) Quenching

5. The boundary surrounding the system is selected to enclose a bulk gas and an unburned gas as shown schematically in Fig. 2. The quench layers on the chamber walls are not part of the system, nor are quench crevices. The quenching process is treated as follows. In an incremental time δt a quench mass δm_q and its associated enthalpy are assumed to leave the system, where

$$\delta m_q = \rho_u \, q \, \psi \quad \delta V_b \tag{1}$$

The quench layer thickness which varies with time is calculated from the relation

$$\frac{q}{q_r} = 0.4 \left(\frac{p}{p_r}\right)^{\alpha} \left(\frac{T_r}{T_u}\right)^{\beta} \tag{2}$$

6. The reference quench conditions (subscript r) and quenching exponents from references [11-14] are given in Table 1. The use of equations (1) and (2) to predict the mass quenched gives reasonable results (as discussed later), even though the model is oversimplified. For example, it is assumed that the mass quenched is independent of the wall temperature and of the turbulent scaling in the boundary layer. These effects and others, which are neglected in the present calculation, are examined in references [15-21].

7. In a manner analogous to quenching on the rotor and housing surfaces, mass is removed from the system when it is compressed into a crevice volume composed of the clearance between the rotor and side covers, and the distance between the rotor face and the first side seal (a volume estimated to be 0.12 cm^3/chamber for the Toyo Kogyo Series 10A engine used in these tests). The mass quenched in this crevice is given by

$$\delta m_c = \rho_u \frac{T_u}{T_w} \frac{A_{q_c}}{A_f} \quad \delta V_b \tag{3}$$

(b) Leakage

8. Gas flow between chambers is estimated by assuming that leakage past the seals may be modeled as the quasi-steady one-dimensional flow of an ideal gas through an orifice of area A_ℓ,

$$\dot{m}_{jk} = A^*_{jk} \quad \rho_j \; a_j \left(\frac{2}{\gamma_j + 1}\right) \tag{4}$$

9. For a choked leakage the effective leakage area and the critical area of equation (4) are synonymous; otherwise the critical area depends upon the pressure ratio across the seal in addition to the leakage area [22]. The determination of the effective leakage area is not a straightforward matter, and the value used in the present calculations (A_ℓ = 0.5 mm^2, or 1 mm^2 per chamber) is an estimate made from measurements of apex seal geometry. Side seal leakage is assumed negligible. Leakage in Wankel engines has been studied by other investigators [23-25]. Whether simple equations such as (4) adequately model the instantaneous leakage rate is not yet clear.

(c) Heat Transfer

10. It is to be expected that energy losses of heat transfer are considerable. Not only does the Wankel possess characteristically large surface to volume ratios compared with an equivalent piston engine, but also large velocity gradients exist at stationary surfaces, since the working fluid is constrained between apex seals and thus forced to rotate at close to the rotor speed. Assuming that the effect of radiation heat transfer on the scaling law is small, then dimensional analysis applied to forced convection suggests that the Nusselt number be some function of the Reynolds number and the Prandtl number. Our study uses the correlations due to Woschni [27] primarily because the expected Reynolds number dependence was displayed,

$$N_u = 0.035 \, Re^{0.8} \tag{5}$$

In the Wankel engine application, we have assumed that the appropriate gas velocity is

$$v = \frac{r\omega}{3} + \frac{c V_d T_o}{p_o V_o} (p - p_m) \tag{6}$$

Equation (5) then adequately models the time average heat losses in the engine [9]. The first term of equation (6) is interpreted as the average gas velocity due to rotor rotation. The second term is an empirical expression included to model the combustion induced gas motion for which Woschni gives $c = 3.24 \times 10^{-3}$ m sec^{-1} °K^{-1}.

11. It is not expected that the equations (5) and (6) will adequately predict the instantaneous heat transfer rate. At close to top dead center, gas velocities are much higher than $r\omega/3$ [7].

12. Using ideal gas models for the burned and unburned gases, and assuming that the volume of burning fluid within the combustion chamber is negligible, the mass fraction burned is related to the cylinder pressure by [9]

$$x = \frac{pV - p_o V_o + (\gamma_b - 1)(W+Q+H) + (\gamma_b - \gamma_u) c_{vu} (m\overline{T}_u - m_o T_o)}{(\gamma_b - \gamma_u) m\, c_{vu}\, \overline{T}_u - (\gamma_b - 1) m (h_{fb} - h_{fu})} \quad (7)$$

The losses which affect the relationship between the mass fraction burned and engine performance parameters are the net heat loss Q and the net enthalpy loss H from the system since ignition. Another way to calculate the mass fraction burned is given in reference [26], however, leakage is neglected.

13. The heat loss correlation, equation (5), is for a system which includes the quench layers. The heat loss from the bulk gas in the system considered here is reduced; since the quench layers are outside the system, a portion of the thermal boundary layer lies outside our open system model of the burned region. Consequently, two limiting cases have been analyzed. The first case assumes that the thermal boundary layer and the quench layer are the same thickness, therefore the bulk gas is adiabatic and Q=0 in equation (7). Since the thermal boundary layer grows with time, it is expected that this assumption will be good early in the combustion phase and break down as time goes on. This expectation leads to the second case where the quench layer is assumed much thinner than the thermal boundary layer so that Q in equation (7) is calculated according to equation (5).

(d) Results

14. Results of calculations of mass fraction burned, based on measured chamber pressure-time curves for a Toyo Kogyo production Series 10A engine are shown in Fig. 3. When x = 1, all the unburned gas available for combustion has been burned. The unburned gas not available for combustion has either been leaked out of the combusting chamber or lies in quench layers and crevice volumes. Only half the leakage is truly wasted, since half of the leakage out of the combusting chamber is into the compressing chamber where it becomes available for the next combustion process.

15. Fig. 3 shows that within the accuracy of our model all the mass has been accounted for, and also that the manner in which the model handles heat transfer is important. The relationship between the quench layer and the thermal boundary layer is clearly an area requiring further study. Order of magnitude calculations using equation (5), Reynold's analogy, and the universal velocity profile suggests that the quench layer thickness is the same order of magnitude as the viscous sublayer. This conclusion depends upon the stoichiometry of the combustion since quenching distance is a strong function of equivalence ratio whereas the boundary layer thickness is not.

16. Table 2 shows the effect of engine speed on the mass balance carried out on the combustion chamber from ignition to end of combustion. The mass available for combustion is about 90 percent and the remaining mass is leaked to the leading or trailing chamber, or is in the quench layers and crevices. Note that the percentage of mass leaked decreases with increasing engine speed.

17. Assuming that leakage, quenching, and crevice volumes are the sources of unburned hydrocarbons (HC) in the Wankel, estimates can be made of the average exhaust HC concentrations using the models already described. These calculations are especially pertinent as they provide a consistency check on the geometrical evaluation of the leakage area.

18. During combustion the leakage out of the chamber is assumed to be unburned gas. This corresponds to assuming that mixing occurs on a time scale long compared to the flame spread, that the flame reaches both apex seals at approximately the same time, and that the effect of the finite thickness of the flame is negligible. The validity of these assumptions are expected to depend upon the number of spark plugs, their position and timing, as well as the parameters governing flame speed.

19. Leakage of unburned gas into the exhausting chamber begins during blowdown and continues until combustion is finished; the integral of the leakage is the leakage contribution to the exhaust HC. Fig. 4 shows a comparison between measured and calculated exhaust HC concentrations. The areas shown crosshatched are the calculated contributions to the total HC concentration of three sources. The calculations assume that once formed the HC does not react since the cases being examined are fuel-rich [28]. At high speeds the quenched HC are the primary source whereas at low speeds the leakage dominates. The crevice volume contribution in this engine appears to be a secondary source.

20. Note that the model outlined calculates heat release rate and predicts HC concentrations which are consistent with experimental observation. One input to the HC calculations which has not yet been mentioned and yet plays an important role in the determining exhaust concentrations is the fraction of the HC formed which is exhausted.

EXHAUST GAS NONUNIFORMITY

21. To examine the distribution of pollutants and fuel-air ratio throughout the exhaust process, a study was completed which time-resolved the exhaust composition and flow-rate [10]. Composition of the exhaust gas, at a given angle, was measured by withdrawing for analysis a small sample at the same point in the exhaust process from successive cycles. This was accomplished by a sampling valve mounted downstream of the exhaust port. By varying the angle at which sampling occurred, the composition was discretely time-resolved. Typical results are given in Fig. 5. Previous investigators [29-31] had shown that nonuniformities in the exhaust flow are significant.

22. Our results show that the exhaust gas can be divided into essentially two phases. First, a leading gas characterized by high concentrations of NO and low concentrations of HC and O_2 concentrations. Nonuniformities in CO and CO_2 are small, slightly higher concentrations being in the leading gas. The leading gas is presumed to be burned gas and quench layers entrained from the rotor face. From these data it has been estimated that 50% of the mass of rotor quench layer is entrained into the exhaust flow during blowdown. The trailing gas is thought to be burned gas, rolled up quench layers, and leakage of unburned gas from the trailing chamber. As the rotor rotates, boundary layers are rolled into vortices by the seals. Assuming only trailing gas remains in the chamber at the end of the exhaust process, the fraction HC exhausted is estimated to be ≃ 90%.

23. It has been tacitly assumed in the performance model that there is no stratification of fuel in the unburned charge. It has long been recognized that the average exhaust composition is a function of the equivalence ratio, thus, it is reasonable to assume that a time resolved equivalence ratio may be calculated from time resolved exhaust composition. The calculations shown in Fig. 5 were done by the method of Spindt [32].

24. Theoretical calculations of the NO gradient in the burned gas, assuming no burnt gas mixing, predict frozen concentrations which are an order of magnitude higher in the first element to burn than in the last to burn [9]. Here a two to one gradient has been measured in the exhaust. The fact that the leading gas is on the average higher in NO than the trailing gas means that on the average the leading gas burns earlier in the cycle than the trailing gas. This is consistent with experimental observations [6, 7] that the flame is assisted in the direction of rotation and impeded in the direction opposite rotation. That a significant gradient in NO has been measured in the exhaust means that mixing in the burned gas is incomplete. That conclusion, coupled to the calculations made of a time resolved equivalence ratio, support the assumption of a homogeneous charge.

PARAMETRIC STUDY OF LOSSES

25. Our thermodynamic model of engine performance can be used to evaluate the relative importance of leakage, heat transfer and quenching on thermal efficiency. To put the real engine cycle in perspective, a comparison was made with a fuel-air cycle calculation [33], and the results are shown in Fig. 6. In the fuel-air cycle the mass inducted into the chamber is the same as in the real cycle, but leakage, heat transfer and quenching are omitted and combustion occurs instantaneously at top-dead center. The real cycle efficiency is about half the ideal fuel-air cycle efficiency, It is also shown in Fig. 6 that losses after combustion, indicative of heat and mass losses, are small. Hence, the greatest loss is due to the finite burning time.

26. The relative importance of leakage, heat transfer and quenching as performance losses was then examined as follows. The experimentally determined pressure-time diagram for the 2000 rpm, mid-load (432 kPa bmep) run was used as input to the performance model previously described. Various assumptions were made about the different loss mechanisms. The spark timing and fuel-air ratio were held constant. The mass inducted was then varied until, at the end of combustion, all the mass in the chamber had been burned, leaked or quenched. The cycle thermal efficiency (which here is inversely proportional to the mass inducted) was then computed. Calculations were carried out with leakage, heat transfer and quench omitted; with these losses included one at a time; and with all losses included. The leakage area was taken at 0.5 mm^2 per apex seal. The results are given in Table 3. Leakage and quenching are comparable in their effect on thermal efficiency; heat transfer is about twice as large at the conditions examined. Note that the inlet mixture temperature varies inversely with the mass inducted with this calculation procedure. The effect of these changes in inlet temperature on brake thermal efficiency is small, however.

27. To determine the effect of reduced leakage due to improvements in seal design on thermal efficiency; a similar series of calculations was carried out with all losses included, but with various leakage areas. The calculated brake thermal efficiencies, as a function of engine speed, are shown in Fig. 7. The A_ℓ = 0.5 mm^2 curve is developed from experimental data (A_ℓ is the leakage area per apex seal); the measured pressure-time curves at each engine speed were then used to calculate the efficiency with different leakage areas. The increasing importance of leakage at lower speeds is clear. These results scale with leakage area, and important realization since the area may be estimated only to order of magnitude and since that area can be expected to vary from engine to engine.

CONCLUSIONS

28. This paper has reviewed a Wankel engine performance model which includes quenching, gas leakage and heat transfer. The validity of the model was demonstrated by comparing a predicted mass balance with measured fuel and air flow rates and hydrocarbon emissions. The model was then used to examine the relative importance of these loss mechanisms on engine brake thermal efficiency. At 2000 rpm, mid-load operation, leakage and quench are comparable in magnitude as performance losses, and about half as large as heat transfer.

ACKNOWLEDGEMENT

29. This work has been supported in part by the National Science Foundation under Grant No. GK-15409, and by General Motors Corporation.

TABLE 1

Quenching Parameters as a Function of Equivalence Ratio ϕ

T_r = 373 °K, p_r = 4 atm

ϕ	q_r (mm)	β	α
.9	.85	.64	.53
1.0	.64	.50	.52
1.1	.56	.50	.62
1.2	.54	.50	.66
1.3	.54	.50	.66

TABLE 2

Mass Balance from Ignition to End of Combustion

Engine Speed RPM	m_o g	m_q/mo %	m_L/m_o %	m_{cv}/m_o %	m_b/m_o %
1000	0.57	2.5	13	0.3	84
1500	0.47	2.6	11	0.4	86
2000	0.44	4.1	7.5	0.3	88
4000	0.42	2.9	5.5	0.6	91
6000	0.49	3.5	2.9	0.5	93

Engine load ≃ 400 kPa

m_o = mass in chamber at ignition

m_q = mass in quench layers

m_L = mass which leaked out of chamber

m_{cv} = mass in crevice volumes

m_b = mass burned during combustion

TABLE 3

Effect of Loss Mechanisms on Thermal Efficiency

Case	Brake Thermal Efficiency η, %	$(1 - \frac{\eta}{\eta_o})$, %
No losses (η_o)	21.9	0
Crevice volume only	21.5	1.8
Wall quench only	20.7	5.5
Leakage only	20.7	5.5
Heat transfer only	19.4	11.4
All losses included	17.0	22.4

2000 rpm, 432 kPa bmep, fuel-air equivalence ratio 1.04

REFERENCES

1. F.V. Bracco and W.A. Sirignano, "Theoretical Analysis of Wankel Engine Combustion," Combustion Science and Technology, Vol. 7 (1973), pp. 109-123.

2. N.C. Blizard and J.C. Keck, "Experimental and Theoretical Investigation of Turbulent Burning Model for Internal Combustion Engines," SAE paper 740191 (1974).

3. G.A. Lavoie, J.B. Heywood, and J.C. Keck, "Experimental and Theoretical Investigation of Turbulent Burning Model for Internal Combustion Engines," Combustion Science and Technology, Vol. 1 (1970), pp. 313-326.

4. P. Blumberg and J.T. Kummer, "Prediction of NO Formation in Spark-Ignited Engines--An Analysis of Methods of Control," Combustion Science and Technology, Vol. 4 (1971), pp. 73-96.

5. F.D. McCuiston, Jr., "An Analytical Evaluation of the Effect of Leakage on NO Emmissions From a Rotary Engine." SAE paper 750023 (1975).

6. I.W. Froede, "James Clayton Lecture--Recent Developments in the NSU Wankel Engine," Proceedings at the Institution of Mechanical Engineers, London, 1965-66, Vol. 180) pt.2A), p. 279.

7. K. Yamamoto and T. Kuroda, "Toyo Kogyo's Research and Development on Major Rotary Engine Problems," SAE Transactions, Vol. 79 (1970), paper 700079.

8. K. Yamamoto, "Rotary Engine and Fuel," paper presented at Eighth World Petroleum Congress, 13-18 June 1971.

9. G.A. Danieli, C.R. Ferguson, J.B. Heywood, and J.C. Keck, "Predicting the Emissions and Performance Characteristics of a Wankel Engine," SAE paper 740186 (1974).

10. C.R. Ferguson, G.A. Danieli, J.B. Heywood, and J.C. Keck, "Time Resolved Measurements of Exhaust Composition and Flow Rate in a Wankel Engine," SAE paper 750024 (1975).

11. R. Friedman and W.J. Johnston, "Pressure Dependence of Quenching Distances of Normal Heptane, Iso-octane, Benzene, and Ethyl-ether Flames," J. of Chemical Physics, Vol. 20 (1952) pp. 919-920.

12. J.T. Agnew and K.A. Green, "Quenching Distances and Propane-Air Flames in a Constant Volume Bomb," Combustion and Flame, Vol. 15 (1970), pp. 189-191.

13. R. Friedman and W.C. Johnston, "The Wall-Quenching of Laminar Propane Flames as a Function of Pressure, Temperature, and Air-Fuel Ratio," J. Applied Physics, Vol. 21 (1950), pp. 791-795.

14. J. M. Ellenberger and D.A. Bowlus, "Single-Wall Quench Distance Measurements," presented at the 1971 Technical Session, Central States Section, Combustion Institute, March, 1971.

15. W.G. Gottenberg, D.R. Olson, and H.W. Best, "Flame Quenching During High Pressure, High Turbulence Combustion," Combustion and Flame, Vol. 7 (1963), pp. 9-16.

16. W.A. Daniel, "Engine Variable Effects on Exhaust Hydrocarbon Composition (A Single-Cylinder Engine Study with Propane as Fuel)," SAE paper 670124 (1967).

17. G. de Soete and A. Van Tiggelen, "Das Abschrecken vorgemischter Flammen durch Parallele Wände," Verbrennung and Feuerungen, VDI-Berichte Nr. 146 (1970), p. 35.

18. A.E. Potter, "Flame Quenching," Progress in Combustion Science and Technology, Vol. 1 (1960), pp. 145-181.

19. J.T. Wentworth, "Effect of Combustion Chamber Surface Temperature on Exhaust Hydrocarbon Concentration," SAE paper 710587 (1971).

20. W.W. Haskell and C.E. Legate, "Exhaust Hydrocarbon Emissions from Gasoline Engines--Surface Phenomena," SAE paper 710587 (1971).

21. V. Panduranga, "Correct Turbulence--A Way to Reduce the Concentration of Unburnt Hydrocarbons From Automotive Engines" Combustion and Flame, Vol. 18 (1972), pp. 461-467.

22. A.H. Shapiro, The Dynamics and Thermodynamics of Compressible Fluid Flow, Ronald Press Co., New York (1935), Vol. I, p. 109.

23. S. Furuhama and E. Omshi, "Study of Gas Leakage on a Rotary Engine," Report, The Musahi Institute of Technology, Department of Mechanical Engineering.

24. M.K. Eberle and E.D. Klomp, "An Evaluation of the Potential Performance Gain from Leakage Reduction in Rotary Engines," SAE paper 730117 (1973).

25. B. Lawton and D.H. Millar, "Leakage and Heat Release in Rotary Piston Engines, Part I: Leakage," The Journal of Automotive Engineering, Vol. 5, No. 3, pp. 15-20.

26. K.C. Tsao and D. Losinger, "Mass Burning Rate in a Rotary Combustion Engine," SAE paper 741087 (1974).

27. G. Woschni, "A Universally Applicable Equation for the Instantaneous Heat Transfer Coefficient in the Internal Combustion Engine," SAE Transactions, Vol. 76, paper 670931 (1967).

28. W.A. Daniel, "Why Engine Variables Affect Exhaust Hydrocarbon Emission," SAE Transactions, Vol. 79 paper 700108 (1970).

29. K. Yamamoto, Rotary Engine, Toyo Kogyo, Japan 1969.

30. K. Yamamoto, T. Muroki, and T. Kobayakawa, "Combustion Characteristics on Rotary Engines," SAE paper 720357 (1972).

31. R.V. Basshuysen, "Air Pollution Control at the Ro 80 Rotary Engine, System NSU-Wankel by Means of a Reactor," Thirteenth FISITA Congress, Paper No. 15.3 B, June 8-11, 1970.

32. R.S. Spindt, "Air-Fuel Ratios from Exhaust Gas Analysis," SAE Transactions, Vol. 74, paper 650507 (1965).

33. C.F. Taylor and E.S. Taylor, The Internal Combustion Engine, International Textbook Co., Penn. (1970)

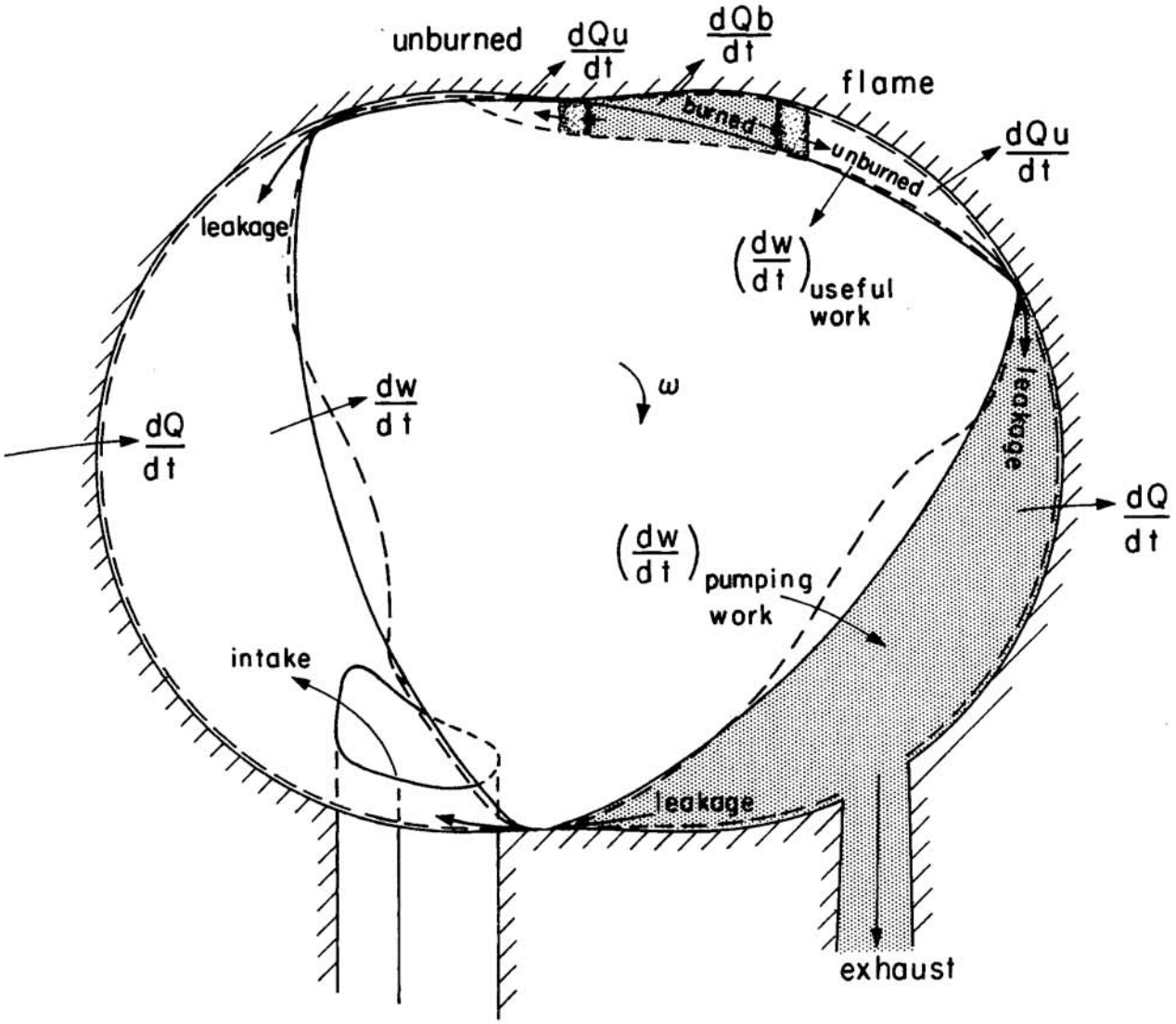

FIG. 1 Schematic of three control volumes, coupled by leakage past apex seals, used to model thermodynamic performance of one rotor.

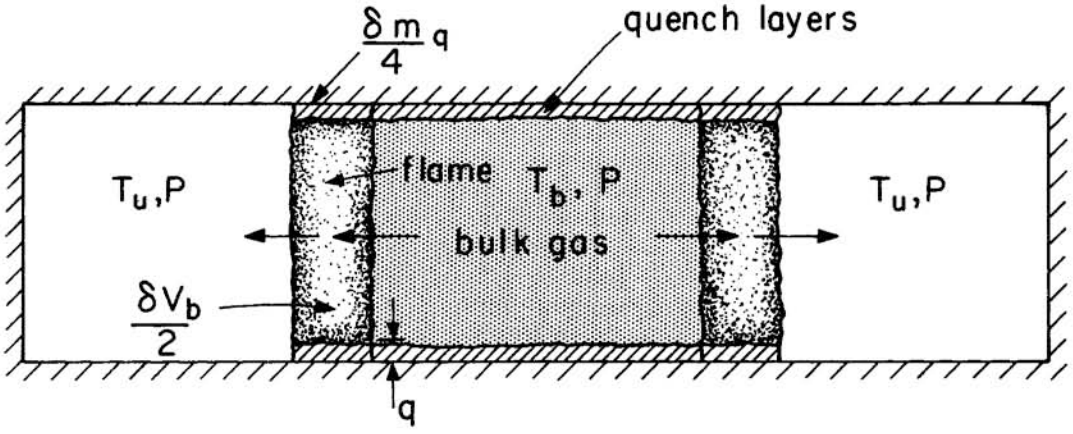

FIG. 2 Simple geometric model for flame quenching at chamber walls.

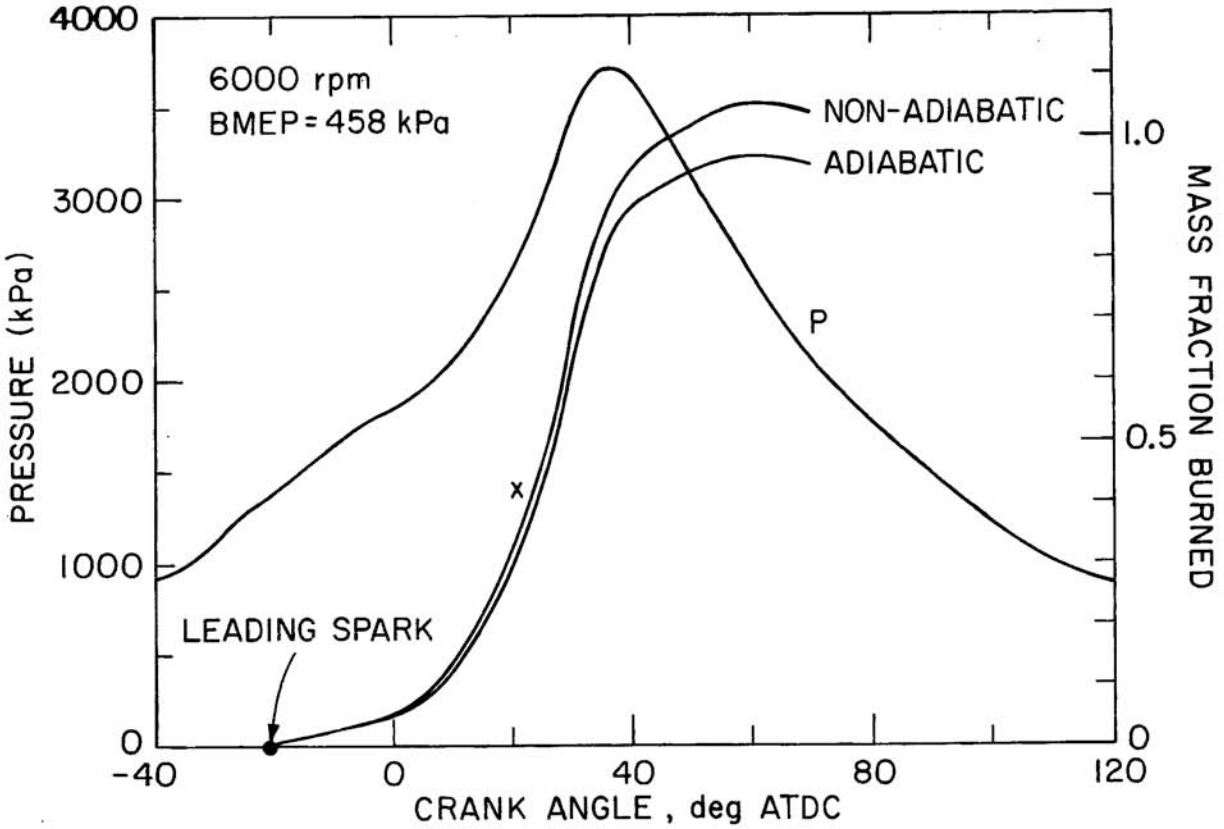

FIG. 3 Measured chamber pressure and calculated mass fraction burned as function of crank angle.

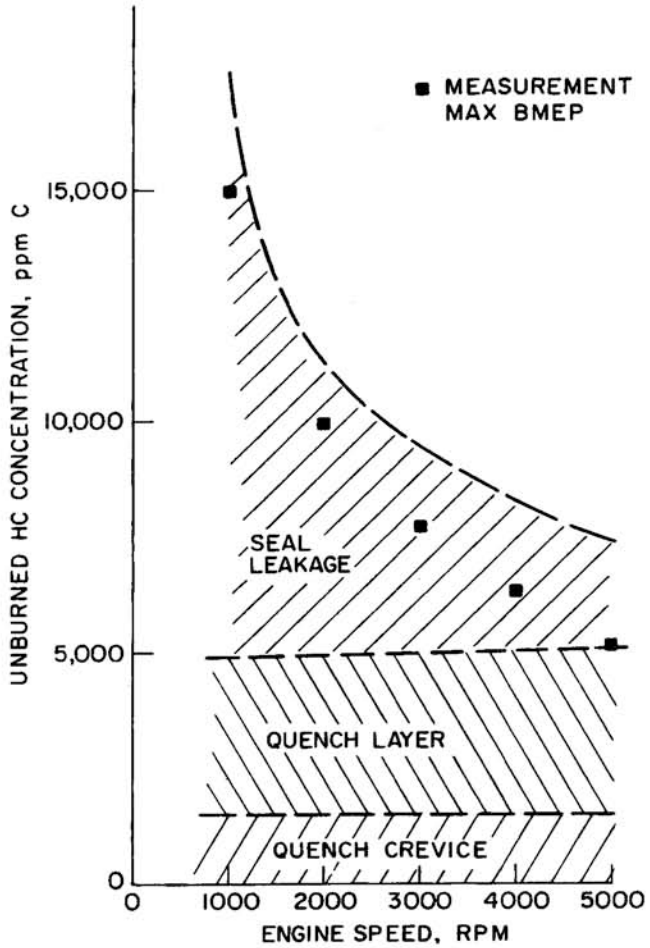

FIG. 4 Measured and predicted exhaust HC concentration at wide-open-throttle, as a function of engine speed.

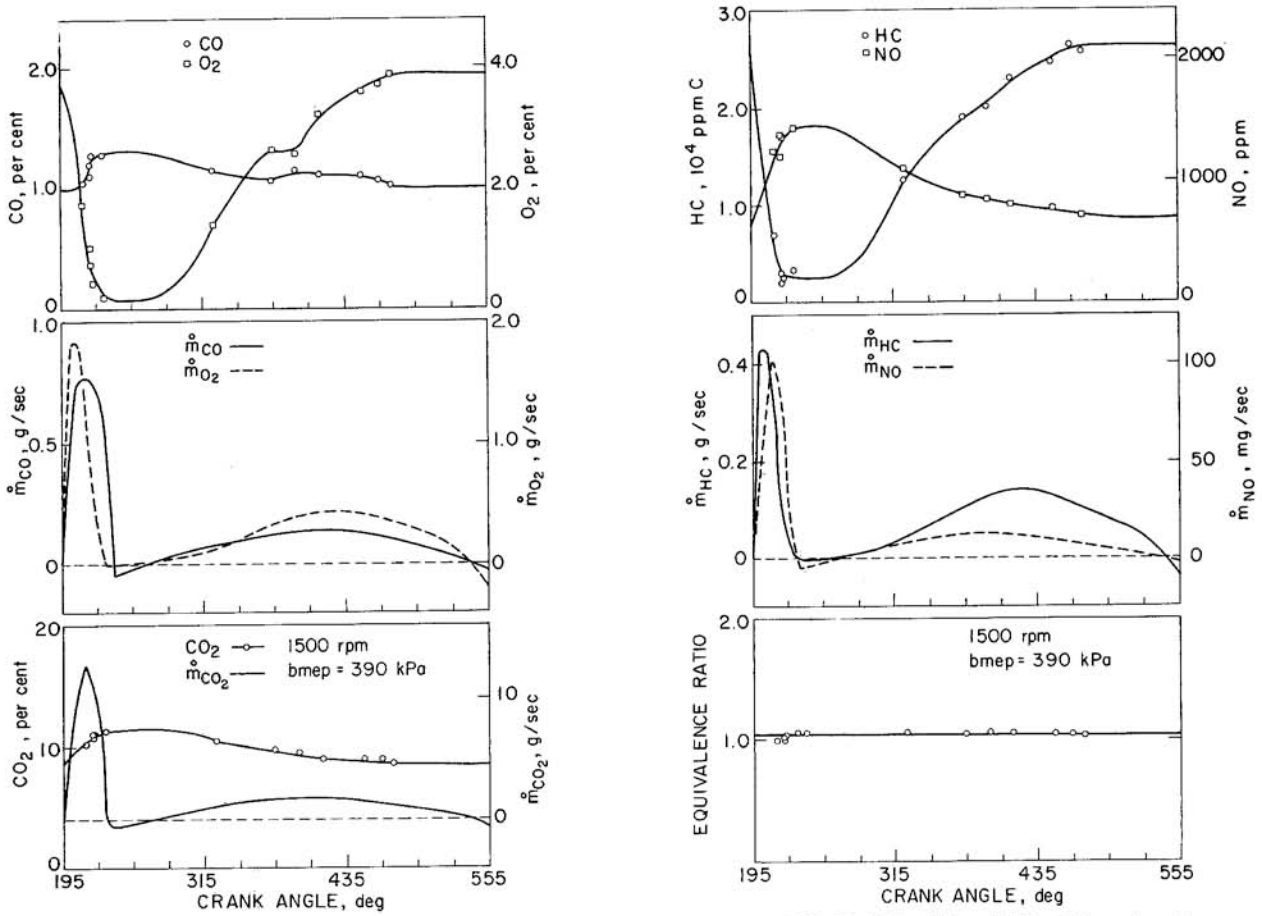

FIG. 5 Time-resolved instantaneous concentrations and mass flow rates of CO, O_2, CO_2, HC and NO at the exhaust port at 1500 rpm, 390 kPa bmep. Calculated instantaneous fuel-air equivalence ratio also shown.

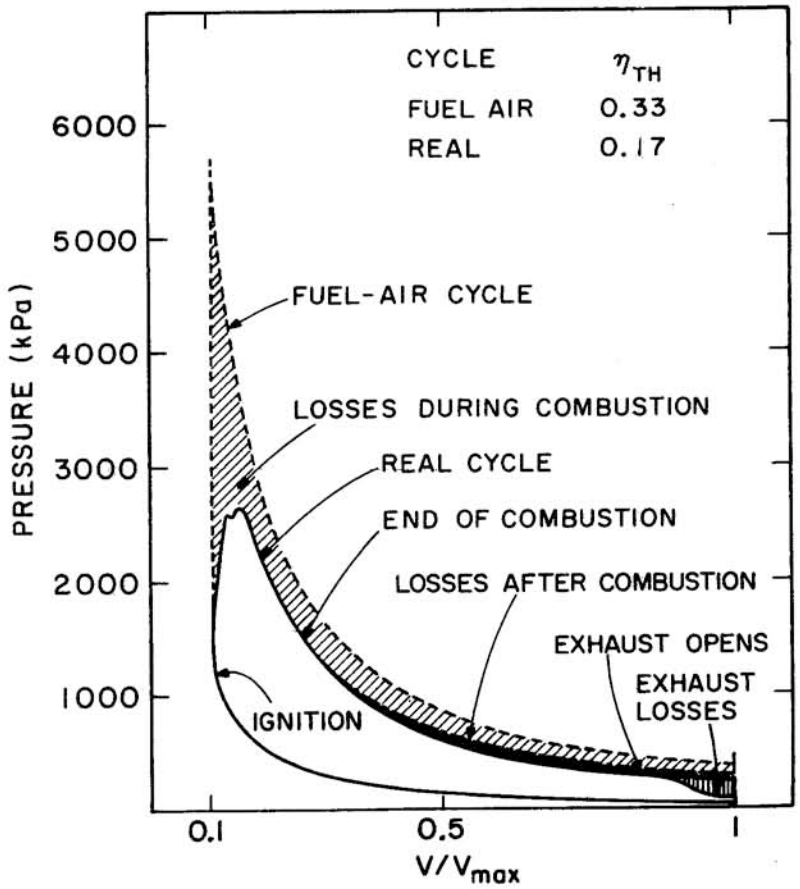

FIG. 6 Comparison of p-V diagram for real engine cycle with ideal fuel-air cycle calculation (at 2000 rpm and 432 kPa bmep for the real cycle). Brake thermal efficiency shown at top-right.

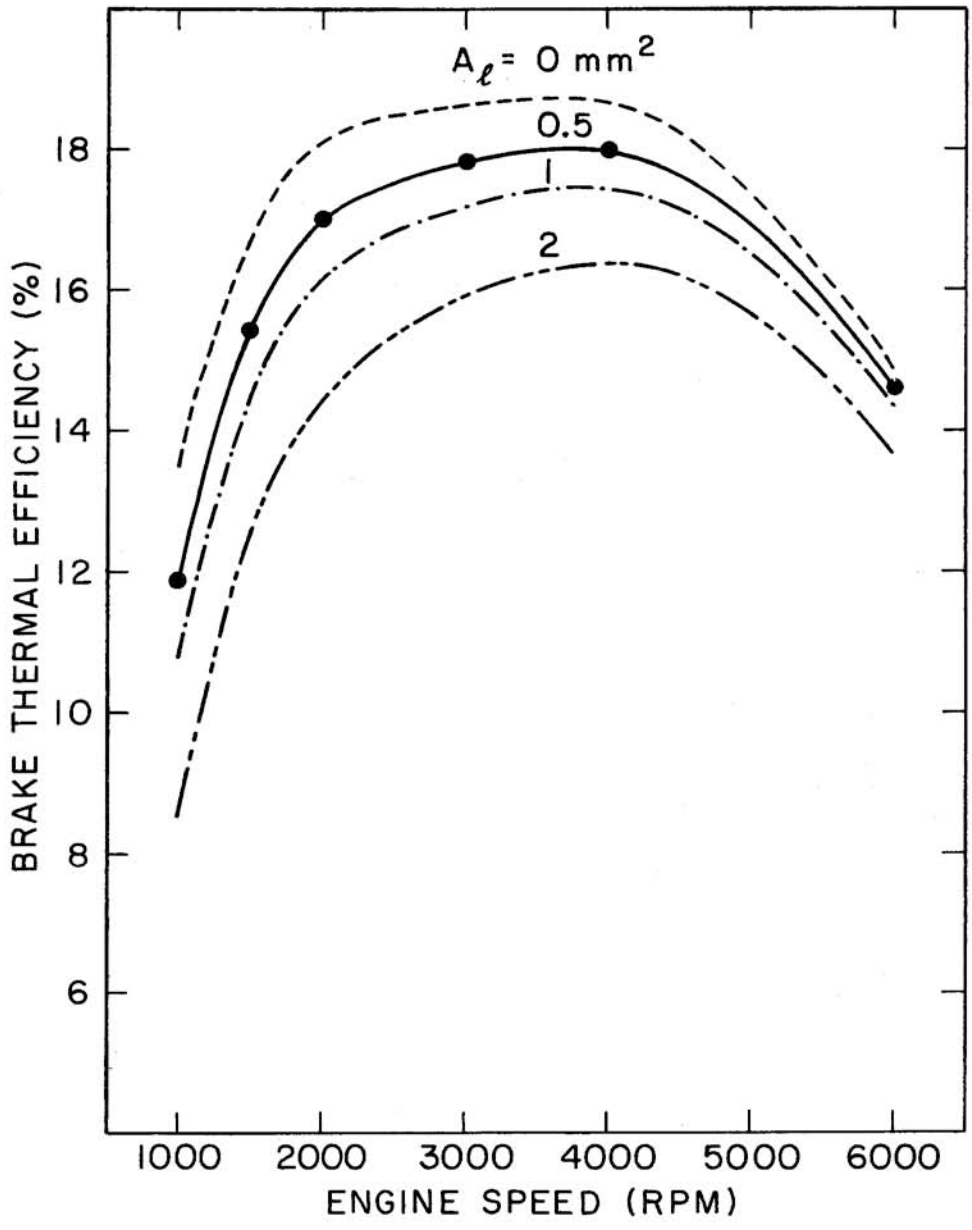

FIG. 7 Calculated brake thermal efficiency at mid-load conditions (350-450 kPa bmep) for various leakage areas, A_ℓ, as function of engine speed.